

- ¹⁶G. P. Mikhailov, D. M. Mirkamilov, Yu. Ya. Gotlib, A. M. Lobanov, and B. Z. Volchek, *Vysokomol. Soedin.* **9**, 1967 (1967).
¹⁷L. J. Garfield and S. E. B. Petrie, *J. Phys. Chem.* **68**, 1750 (1964).
¹⁸H. Oberst, *Kunststoffe* **53**, 4 (1963).
¹⁹J. Heijboer, *J. Polym. Sci. C* **16**, 3755 (1968).
²⁰J. Bussink and J. Heijboer, in *Physics of Non-Crystalline Solids*, edited by J. A. Prins (Wiley, New York, 1965).
²¹J. Heijboer, L. C. E. Struik, H. A. Waterman, and M. P. Van Duijkeren, *J. Macromol. Sci. Phys.* **5**, 375 (1971).
²²R. M. Fuoss, *J. Am. Chem. Soc.* **63**, 378 (1941).
²³J. D. Ferry, *Viscoelastic Properties of Polymers* (Wiley, New York, 1961).
²⁴R. M. Mininni, R. S. Moore, and S. E. B. Petrie, *Bull. Am. Phys. Soc.* **17**, 373 (1972).
²⁵J. Heijboer in Ref. 20.
²⁶M. Baccaredda, E. Butta, and R. Caputo, *Chim. Ind.* **40**, 356 (1958).
²⁷D. J. Massa (unpublished).
²⁸K. H. Illers and H. Breuer, *Kolloid-Z.* **176**, 110 (1961).
²⁹F. Krum and F. H. Muller, *Kolloid-Z.* **164**, 81 (1959).
³⁰T. Hara, *Jap. J. Appl. Phys.* **6**, 147 (1967).
³¹L. J. Garfield, *J. Polym. Sci. C* **30**, 551 (1970).
³²S. Matsuoka and Y. Ishida, *J. Polym. Sci. C* **14**, 247 (1966).
³³G. Locati and A. V. Tobolsky, *Adv. Mol. Relax. Processes* **1**, 375 (1970).
³⁴N. G. McCrum, B. E. Read, and G. Williams, *Anelastic and Dielectric Effects in Polymeric Solids* (Wiley, New York, 1967), p. 409.
³⁵O. Yano and Y. Wada, *J. Polym. Sci. A-2*, **9**, 669 (1971).
³⁶J. Heijboer, *Kolloid-Z.* **171**, 7 (1960).

Morphology of strain-induced crystallization of natural rubber. I. Electron microscopy on uncrosslinked thin film

D. Luch* and G. S. Y. Yeh

Department of Chemical Engineering, Department of Materials and Metallurgical Engineering and the Macromolecular Research Center, The University of Michigan, Ann Arbor, Michigan 48104

Pt shadowing, Au decoration, OsO₄ staining, electron diffraction, and bright- and dark-field electron microscopy have been used to elucidate strained and unstrained thin-film morphology of natural rubber. Unstrained natural rubber exhibits a 100–150-Å nodular morphology in the melt at room temperature. When cooled below room temperature, the original nodular morphology is replaced by an unoriented lamellar morphology. The crystal thickness of the lamellae is about 55 Å at –28 °C. When stretched to elongations greater than about 200% the strain-crystallized films show a distinct fibrillar morphology at room temperature. The fibrils appear to be composed of individual crystallites, 120 Å in diameter. When cooled to –25 °C, including those films which have been highly stretched (900%), the original fibrillar morphology is replaced by an oriented lamellar morphology. The transformation to lamellar morphology involves a lateral alignment of the room-temperature crystallites and a decrease in crystal thickness. Upon heating above –25 °C, the lamellar crystals thicken and lamellar periodicity increases, but eventually the structure reverts to the fibrillar form as room temperature is approached, indicating the reversible nature of the morphological transformation.

INTRODUCTION

Crystallization of polymeric materials subjected to flow and/or elastic strain fields frequently occurs in fabrication processes. Consequently, elucidation of the influence of strain on the morphology and the mechanism of polymer crystallization is of considerable technological importance.

Two publications on the morphology of strain-induced crystallization, one by Keller and Machin¹ on polyethylene from the rubbery melt state and the other by Yeh and Geil² on polyethylene terephthalate from the glassy amorphous state, have led to apparent differences in conclusions concerning the mechanism of strain-induced crystallization.

The differences are primarily due to the differences (apparent or real) in the morphology revealed by the two respective studies. Keller and Machin show essentially a perpendicularly oriented shish-kebab-type lamellar morphology as previously shown by Kobayashi in a blown polyethylene film,³ whereas Yeh and Geil reveal the presence of a nodular structure (~100 Å) within perpendicularly oriented "lamellae". It is not clear how much of the observed differences in morphology is due to polymer, specimen preparation, and/or resolution, and how much is attributable to the difference in physical state (melt or glass) from which the two oriented polymers were crystallized.

Based on the similarity in morphology in polyethylene, gutta percha,¹ natural rubber,⁴ and the shish-kebab-type structures observed in solution-grown stirred-crystallized polyethylene,⁵ Keller and Machin proposed a two-step nucleation and growth mechanism for crystallization

under orientation. The mechanism is basically describable in terms of a shish-kebab structure supposedly consisting of extended-chain shish and folded-chain kebabs. The nucleation process is thought to be associated with the formation of extended-chain crystals from oriented molecules and the growth process is thought to be associated with the formation of lamellar crystals from an isotropic melt by chain folding onto the line nuclei. There are two major problems with this proposed crystallization mechanism: the evidence for the extended-chain line nuclei and the chain folding during crystal growth.

In the past the evidence for extended-chain crystals came primarily from the melting behavior which showed a higher melting point at about 140 °C for polyethylenes crystallized from either an oriented melt or a stirred solution.¹ However, the higher melting point can also be attributed to other factors such as the presence of tie molecules which increase with increasing extensions.⁶ Recent gel permeation studies,⁷ and, more definitively, dark-field electron microscopic studies⁸ also question the presence of extended-chain crystals in solution-grown polyethylene by stirring. Furthermore, dark-field studies of natural rubber crystallized by stretching without further supercooling also do not reveal any crystals more than 100–200 Å along the *c* axis.⁹

The suggested crystal-growth process by molecules chain folding onto oriented line nuclei to explain the observed lamellae should ordinarily lead to an increase in axial stress during crystal growth. Experimentally Gent¹⁰ reported complete axial stress relaxation in bulk natural rubber for conditions (elongation, crystallization temperature, etc.) similar to those at which Andrews⁴

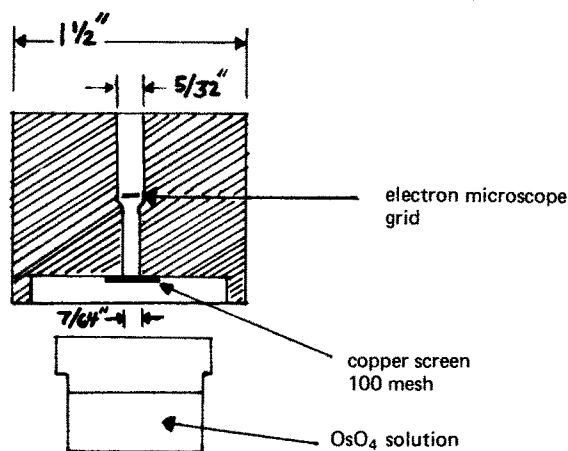


FIG. 1. OsO_4 staining capsule.

reported the oriented lamellae in thin natural rubber films. Indeed, Gent¹¹ had concluded in one of his papers that "the form and magnitude of the stress changes during the crystallization of stretched networks of trans-polyisoprene are generally similar to those observed for cis-polyisoprene,¹⁰ cis-polybutadiene,¹² and trans-polychloroprene¹³ networks. They are in accord with the suggested formation of bundle-type crystallites oriented in the direction of extension to various degrees". Thus, based on axial stress-relaxation evidence, Gent ruled out the possibility of chain folding *during* oriented crystallization. However, there is very little question concerning the presence of folded-chain lamellar structures in stretched natural rubber. Our own freeze-fractured surfaces of strain-crystallized natural rubber showed well-defined lamellar structures oriented perpendicular to the stretch direction.¹⁴ Therefore, one has now the obvious paradox of stress relaxation occurring while the folded-chain lamellae are being formed (apparently requiring chain folding) during oriented crystallization. The paradox did not arise in the case of strain-induced crystallization from the glassy state for polyethylene terephthalate since Yeh and Geil were able to show that the crystallization process results primarily from orientation, crystallization, and rearrangement of partially *prefolded* nodules originally shown to be present in the glassy amorphous state.¹⁵ The same crystallization mechanism also appears to be operating in plasticized rubbery isotactic polystyrene when crystallized under high extensions.¹⁶ In both studies,^{15,16} dark-field studies do not reveal any extended-chain crystals of dimensions greater than 100–200 Å in the *c* axis. However, no similar fine structures have been reported by Andrews and Reeve,¹⁷ and it is not known to what extent the results obtained with the glassy or plasticized "rubbery" materials can be directly compared with crystallization from the strained melt.

In an attempt to obtain additional information about the questions of crystal nucleation and growth from strained polymer melts, we have gone back to natural rubber and taken on a comprehensive study of its morphology as well as its stress-relaxation behavior. The results are presented in three parts: Part I presents the results of electron microscopy performed on thin films of natural

rubber, examined at elongations from 0 to 900% and at temperatures from -25 to $+55$ °C. Part II presents the results of x-ray studies on bulk crosslinked natural rubber specimens, for which small- and wide-angle scattering has been determined over a temperature range from -25 to $+25$ °C and for elongations of 0, 100, and 700%. Part III presents the results of axial stress relaxation measurements made on strained natural rubber at temperatures between -25 and 0 °C. In addition, part III discusses the composite picture formed by the results of the three independent experimental investigations.

Natural rubber was chosen not only because of our earlier work on its strain-induced crystallization morphology but also because it has a reported isotropic melting point of about 28 °C for which stretching of the rubbery melt can be conveniently carried out at room temperature. The double bond in natural rubber also allows chemical staining and permanent fixing with OsO_4 , which becomes particularly suitable for direct measurements of crystal and amorphous thicknesses.

In this paper thin-film morphology is examined using a variety of specimens including those that have been Pt shadowed, Au decorated, or OsO_4 stained.

EXPERIMENTAL

In all cases rubbery films were mounted on support films having a network of very small holes of diameter approximately 0.2 – 2.0 μ , thus permitting reduction of specimen thickness to a practical minimum and ensuring maximum microscopic resolution. Examination was made on those parts of the film covering the holes. Preparation of these microgrid support films is described elsewhere.¹⁸

Rubber films, estimated to be about 500 Å thick, were formed by placing a few drops of a 1.8% solution of pale crepe in benzene on the surface of distilled water and allowing the benzene to evaporate. (In some cases, referred to later, films were initially cast from solution onto a glass slide then floated off onto water.) Stretched films were prepared by stretching the thin rubber film directly on the water surface using a pair of modified draftsman's dividers.² Mounting was done by placing microscope grids, previously covered with a microgrid

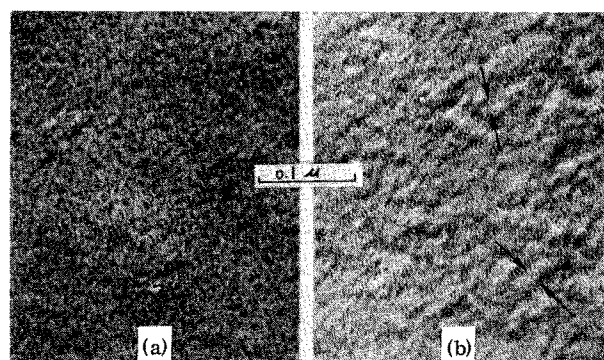


FIG. 2. Pt-shadowed thin films of unstrained natural rubber showing a nodular texture indicated by arrows. (a) Casted on water. (b) Casted on glass slide.

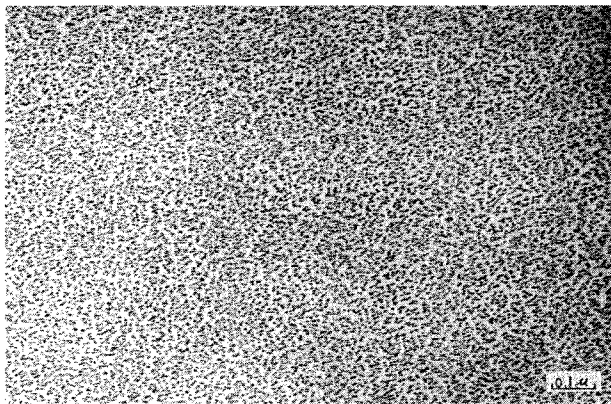


FIG. 3. Au-decorated thin film of unstrained natural rubber.

support, on the rubber film and using a fine metal screen to "sweep" the grids and rubber film off the water surface. In some cases the stretched thin rubber films were conditioned for comparison with the unconditioned samples by immersing the specimen grid directly into nitrogen at 75 °C for 10 sec. This conditioning procedure was designed to remove possible nonequilibrium effects associated with the original film preparation. In almost all cases the rubber films were subjected to additional treatment in order to enhance contrast and/or explore structural features. Platinum shadowing and gold decoration¹⁹⁻²¹ were done by methods developed earlier. OsO₄ (osmium tetroxide) staining had the combined effect of imparting increased contrast and the fixation of structural features.⁴ Therefore, staining of films at low temperature caused retention of the crystalline-amorphous composite texture when the film was examined at room temperature. OsO₄ staining was done by exposing the rubber film for 5 min to the vapor above a 2% solution of OsO₄ in water. However, in order to allow staining at controlled temperatures other than room temperature, specimen grids were placed in the staining capsules pictured in Fig. 1 during thermal treatment. These cylindrical aluminum capsules had an over-all diameter of 1½ in., with holes of $\frac{5}{32}$ and $\frac{7}{64}$ in. drilled alternately from either end along the cylindrical axis and meeting approximately at the capsule center. The specimen on a standard 3-mm electron microscope grid rested at the center of the capsule which served as a large thermal capacitor. In order to minimize the effects of convection currents when staining, the smaller hole at the bottom of the cylinder was covered with fine copper mesh while the larger hole at the top was covered with Scotch tape. Continuous temperature variation from -28 °C to room temperature was achieved by placing these capsules in a controlled cold-air bath, for which temperature fluctuation was in all cases less than ± 0.5 °C. Staining was done within the cold-air bath by placing the capsule over a 1.0-in.-diameter bottle containing the OsO₄ solution, also shown schematically in Fig. 1.

A JEM-6A electron microscope was used for this study and in most cases samples were examined at room temperature.

RESULTS

Unstretched films

Room temperature. Figs. 2(a) and 2(b) show micrographs of unstretched noncrystalline natural rubber films which were platinum shadowed at room temperature (28 °C). The water-cast film [Fig. 2(a)] has a nodular surface structure of relatively poor definition and contrast and highly variable dimensions but with the center-to-center nodular spacing usually falling between 100 and 140 Å.

In films initially formed on a glass slide [Fig. 2(b)] the surface texture is much better defined, with a center-to-center nodular spacing of 110 to 160 Å, generally larger than for the water-cast films. These nodules are similar to the structures previously observed for polyethylene terephthalate¹⁵ which were interpreted as partially folded molecular bundles having paracrystalline-type chain ordering. The structures in amorphous rubber films are expected to be more perfected in slide-cast films for which the rate of solvent evaporation (drying time) is an order of magnitude less than in the water-cast films.

Figure 3 is a micrograph of an unstretched water-cast film which was gold decorated and examined at room temperature. Close examination of this figure reveals that many regions, between 100 and 200 Å in size, are

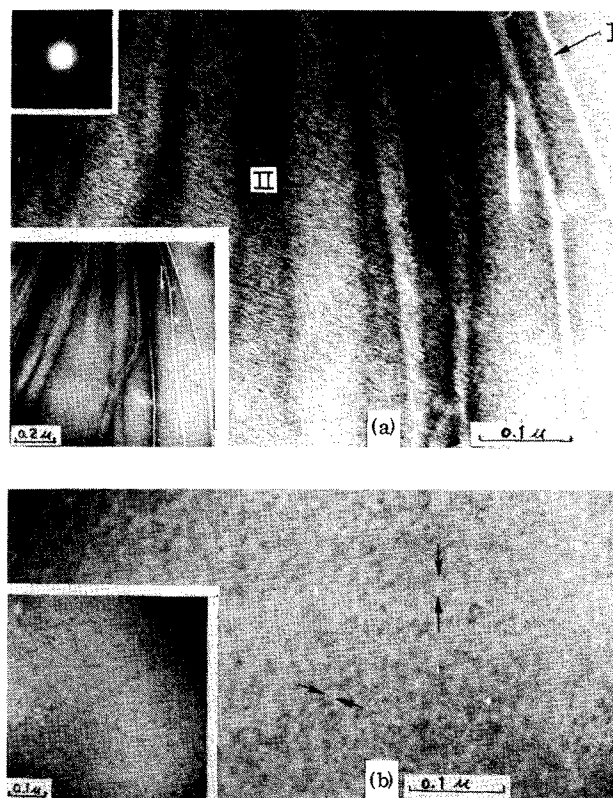


FIG. 4. Unstrained natural rubber crystallized 15 days and OsO₄ stained at +5 °C. (a) Crystalline lamellae oriented perpendicular (I) and near parallel (II) to surface. Inset shows a diffraction pattern from type-II crystalline orientation. (b) Nodular area. Arrows indicate nodular structure.

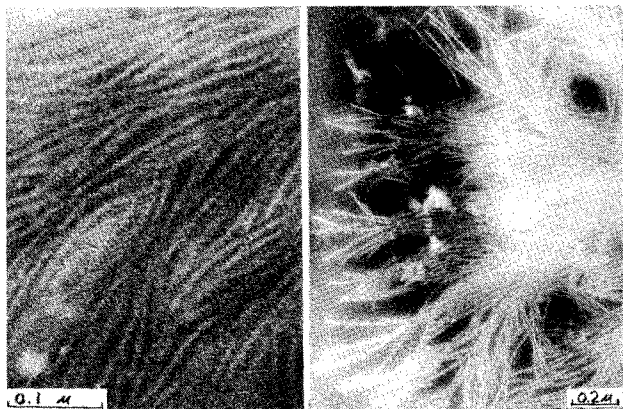


FIG. 5. Unstrained natural rubber crystallized 13 h and OsO_4 stained at -28°C .

completely void of gold particles. Although the gold decoration on unstretched films always appears to be somewhat ordered in the sense of voiding certain regions, the average size of voided areas exhibited by various films of nominally identical preparation is not always the same, but varies between 125 and 175 Å for any particular film. This room-temperature gold decoration of unstretched films indicates a surface heterogeneity of dimension similar to the structure observed for the platinum-shadowed films.

Unstretched films which have been lightly stained with OsO_4 vapor at room temperature (30-sec exposure) also show evidence of a structure averaging some 150 Å in diameter. In this case structural contrast is poor, probably due to the inability of the severe OsO_4 stain to make anything but a truly crystalline-amorphous distinction. In a separate independent study, the structures seen in unstretched films have a nematic liquid crystalline order.²²

Low temperature. Figure 4(a) shows a portion of a spherulite in an unstretched natural rubber film held 15 days at $+5^\circ\text{C}$. One immediately observes that there is very little coordination between the orientations of neighboring lamellar structures. Some of the crystalline lamellae are seen edgewise (I) and measure 60–85 Å in thickness while some neighboring lamellae (II) appear to lie flat in the plane of the film and have variable length and width dimensions. These flat lamellae are characterized by an irregular darker fringe separating apparent crystalline material from adjacent amorphous areas. Electron diffraction patterns obtained from these flat lamellae, shown in the inset, are of a single-crystal spot type showing 120 and 200 reflections. The positions of the reflections, and the fact that no (hkl) reflections with $l \neq 0$ are seen, indicate that the chains in these flat lamellae are perpendicular to the plane of the film. Since the film has an estimated thickness of less than 500 Å and the rubber molecules have a very high molecular weight (typically $>500\,000$), a significant number of chains must fold back within the lamellae. This is similar to the conclusion reached much earlier by Storcks from electron diffraction studies of crystallized rubber films.²³

Figure 4(b) shows an area which has not yet crystallized, at least in the lamellar form, from the unstretched film held at the same temperature, $+5^\circ\text{C}$ for 15 days. A distinctly beady structure appears, with the diameter of the individual beads varying from 70 to 150 Å, averaging about 110 Å. Such areas do not show a crystalline electron diffraction pattern. Figure 5 shows a portion of a spherulite in an unstretched film held 13 h at -28°C , near the temperature of maximum crystallization rate.²⁴ Many areas are observed in which the crystalline lamellae are oriented primarily edgewise to the plane of the film. The thickness of these lamellae varies between 45 and 75 Å, generally less than the thickness of the lamellar edge measured for crystallization at $+5^\circ\text{C}$. In addition, it was noted during examination in the electron microscope that OsO_4 staining generally produces less crystalline-amorphous contrast in samples crystallized at -28°C as compared with crystallization at $+5^\circ\text{C}$. This indicates either decreased reactivity or decreased penetrability of the stain in amorphous regions with decreasing temperature.

Figure 6 is a micrograph of an unstretched film which was gold decorated first at room temperature, afterwards crystallized at -28°C , and then OsO_4 stained at -28°C . Gold particles were observed along the edges of the developing lamellar core as indicated by the arrows in this figure. This alignment is apparent only in those areas where lamellae had developed edgewise to the film plane. The gold particles are usually about 45 Å in size and the separation between rows of particles is about 60 Å, the approximate thickness of the crystalline core. Making the reasonable assumptions that (a) the gold particles are actually following the movement of material during the crystallization process at lower temperature and (b) there is little mobility of the gold particle itself on rubber film at room temperature, comparison of Figs. 3 and 6 indicates that the crystalline lamellar core is formed primarily of material originally voided of gold at room temperature before crystallization. The two assumptions concerning gold particle movement are further borne out, in some sense, with OsO_4 staining.

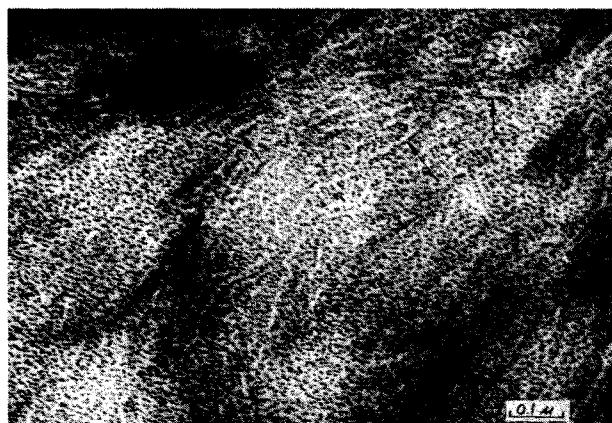


FIG. 6. Unstrained natural rubber Au decorated at room temperature and then crystallized 13 h and OsO_4 stained at -28°C . Arrows indicate presence of lamellae oriented perpendicular to surface.

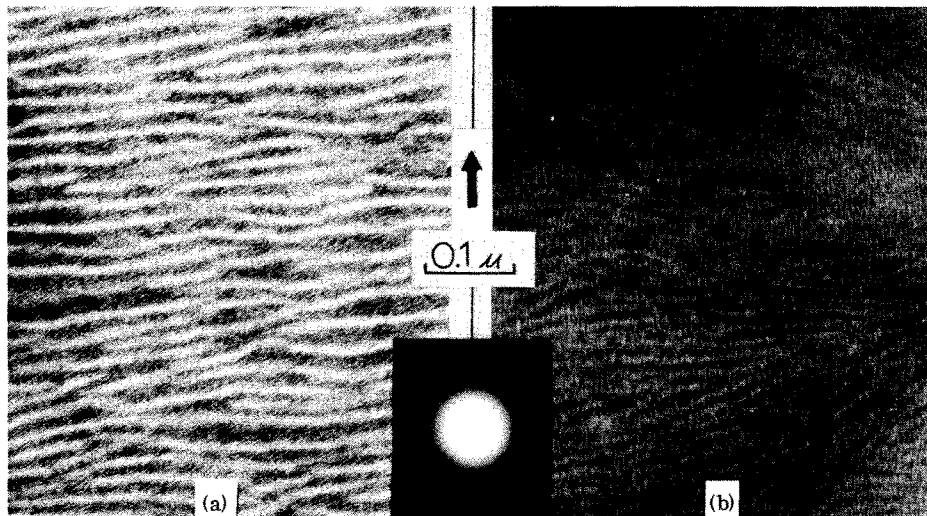


FIG. 7. Natural rubber strained 100%, crystallized, and OsO_4 stained at low temperature. (a) Crystallized at $+5^\circ\text{C}$ for 15 days. (b) Crystallized at -28°C for one day. Inset is diffraction (from sample crystallized at $+5^\circ\text{C}$) showing c -axis orientation in the vertical direction. (Arrow indicates stretch direction in this and subsequent micrographs.)

Stretched films

Thin films of natural rubber stretched on a water surface do not draw uniformly, undoubtedly because of some thickness variations in the film. Although in the following sections the degree of elongation is specified by the macroscopic strain, it should be remembered that this represents only a qualitative measure of sample elongation. The characteristic morphology of stretched films, as deduced from numerous experiments, will be discussed according to the degree of elongation in three parts: low elongation of 100–200%, medium elongations of 250–450%, and high elongations of 500–900%.

Films stretched to 100–200%

Room temperature. At room temperature the lightly stretched films are indistinguishable from unstretched films as revealed by gold decoration and OsO_4 staining. No crystalline electron diffraction is seen for low elongations at room temperature.

Low temperature. Figures 7(a) and 7(b) show the effect of crystallizing a specimen strained 100% at $+5$ and -28°C , respectively. Film A is osmium stained at $+5^\circ\text{C}$ after holding 15 days, while film B was held at -28°C one day before staining. Both films exhibit a distinctly lamellar crystalline structure in which the lamellar crystals have developed perpendicularly to the strain axis and appear predominantly in the edgewise position. The electron diffraction pattern seen in the inset from these crystallized films shows a preferred orientation of the chain axis coincident with the strain axis, indicating that the chains are aligned parallel to the normals of the lamellar crystals (the electron diffraction pattern shown is from the sample crystallized at $+5^\circ\text{C}$; electron diffraction patterns from samples crystallized at -28°C are qualitatively identical, but in general the reflections are much less intense). It will be reported in part II that this pattern is very similar to wide-angle x-ray patterns from bulk samples strained 100% and then frozen at low temperatures. However, there are major differences caused by freezing at $+5^\circ$ as compared with -28°C . First, the crystalline-amorphous contrast, as revealed by OsO_4 staining, is lower at -28 than at $+5^\circ\text{C}$. Second, the crystalline core thickness for the

$+5^\circ\text{C}$ sample varies between 65 and 80 \AA , while for the -28°C sample this core size measures 45–60 \AA . Similar differences have already been noted for unstretched material. Finally, the longitudinal periodicity for the sample at $+5^\circ\text{C}$ is 200–230 \AA , but at -28°C this periodicity is 130–160 \AA . It will be mentioned in part II that these values for long periodicity are comparable to the long spacings determined by direct application of Bragg's law to discrete small-angle x-ray diffraction peaks from samples strained 100%, which are 196 \AA for crystallization at -2°C and 138 \AA for crystallization at -25°C .

It should be mentioned at this point that the lamellar structures which develop at low temperatures for the 100% strain *occasionally* appear to nucleate and grow from some central thread elongated in the stretch direction (none shown in Fig. 7) resembling the shish-kebab-type structures reported by Andrews. However, as often as not the lamellar texture appears to have developed independently of any observable common line nucleus.

Films stretched to 250–450%

Room temperature. Films strained to intermediate elongations of 250–450% generally show a fibrillar crystalline texture associated with highly strained (500–900%) natural rubber at room temperature; but the number of fibrils are distinctly fewer for the lower elongations.

Figures 8(a) and 8(b) show typical micrographs from a film stretched 300% and OsO_4 stained at room temperature. The fibrous texture is discontinuous, composed mainly of nodular crystallites some 100 \AA in diameter. A discontinuous fibrillar morphology was also noted earlier by Andrews²⁵; its exact cause, however, was not established. In some rare cases fibrils appear continuous [Fig. 8(a)] along the strain axis (as judged by OsO_4 staining) for distances up to about 0.2 μ . However, the predominant texture is definitely discontinuous along the strain axis which agrees with the results from earlier dark-field studies by Yeh.⁹ A dark-field electron micrograph obtained from a 400% stretched thin film is shown here in Figure 8(c).

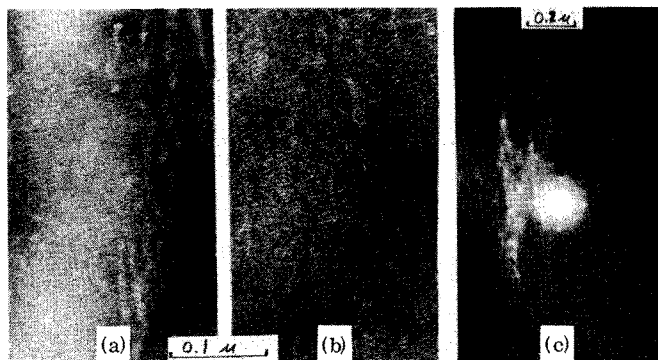


FIG. 8. Strained natural rubber. (a) and (b) Strained to 300% and OsO_4 stained at room temperature. (c) Dark-field electron micrograph obtained from an unstained 400% stretched sample. It was taken using both the (200) and (120) reflections. The electron diffraction is superimposed on the dark-field micrograph.

Low temperature. When a rubber film strained 250–450% is held at -28°C for periods of greater than 1 h, a lamellar texture similar to that observed at 100% strain [Fig. 7(b)] develops, with a lamellar crystalline core thickness of 55 \AA and a longitudinal periodicity of about 135 \AA .

Morphological changes on heating the lamellar crystalline film. A number of specimens strained 300% were placed at -28°C for 40 h to produce the lamellar texture and then heated at a rate of $0.1^\circ\text{C}/\text{min}$ until room temperature was reached. Samples were stained at various temperatures during this heating in order to preserve the thermally induced microstructural changes. In all cases lamellar textures were observed up to a temperature of about 0°C , although minor annealing effects were reflected in increased lamellar clarity and contrast with increasing temperature. Above about 0°C however, large-scale crystalline melting began. For example, Fig. 9(a), a micrograph of the film stained when the temperature reached $+10^\circ\text{C}$, shows that much of the lamellar material has disappeared, leaving only short segments whose thickness appears to have increased slightly to 75 \AA . Close inspection of Fig. 9(a) for the sample strained 300% at $+10^\circ\text{C}$ also suggests the presence of fibrous threads running parallel with the strain axis and composed of two or three strings of tiny crystallites some $65\text{--}90 \text{ \AA}$ in diameter. Further heating above $+10^\circ\text{C}$ [Fig. 9(b), $+13^\circ\text{C}$] leads to further melting of the lamellae and return to a fibrous crystalline texture. All evidence of the lamellar structure is lost as room temperature is reached.

Films stretched to 500–900%

Room temperature. Figure 10 shows the typical morphology of a highly stretched thin film, this one being strained 700% at room temperature and stained immediately with OsO_4 . The texture is very particulate, with small nodular crystallites (lighter areas) having an apparent crystalline core diameter of $100\text{--}130 \text{ \AA}$. The crystallites occasionally show a tendency to align somewhat in the stretch direction, although such alignment does not appear to be a necessary characteristic of the room-temperature texture in highly stretched films.

The electron diffraction pattern from the sample strained 700% at room temperature is shown in the inset of Fig. 10. It is similar to wide-angle x-ray patterns obtained at room temperature from bulk samples strained 700% (see part II) and shows a high degree of chain-axis alignment in the stretch direction. The fact that the electron diffraction pattern from thin films strained 700% exhibits only a weak (120) reflection indicates a preferred orientation of the a crystallographic axis in the plane of the film. Preferred orientation of the a axis in stretched natural rubber has been shown²⁶ to be characteristic of large sample-width-to-thickness ratios, a situation which certainly exists for the thin film.

Aging stretched films (700%) for periods up to five months at room temperature under vacuum results in a slight increase in definition of the nodular crystallites but with no detectable change in size. In addition, such room temperature aging results in a slight tendency for the particulate crystallites to align *laterally* perpendicular to stretch.

Above room temperature. The effect of increasing temperature was also studied by heating films initially strained 700% at room temperature for 2 min at temperatures up to 55°C and then staining at the elevated temperature. In general, increasing temperature results

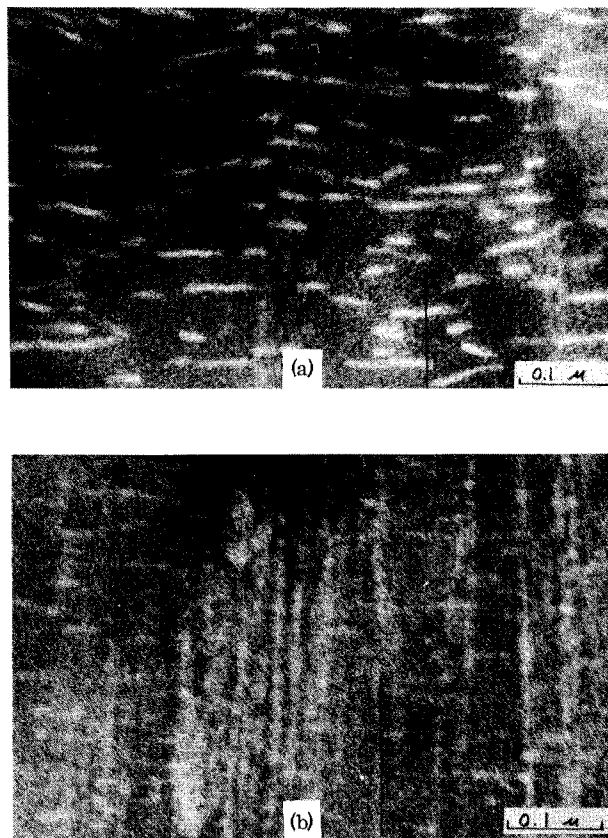


FIG. 9. Natural rubbers strained to 300%, crystallized at -28°C for 40 h, then heated at $6^\circ\text{C}/\text{h}$. (a) OsO_4 stained at $+10^\circ\text{C}$. (b) OsO_4 stained at $+13^\circ\text{C}$.

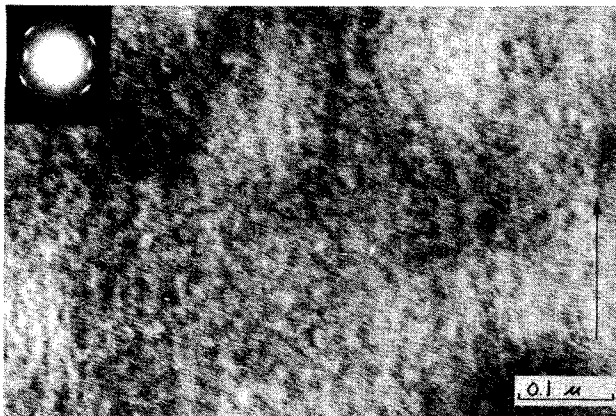


FIG. 10. Natural rubber strained 700% and stained immediately with OsO_4 at room temperature.

in a decrease in the degree of crystallinity as judged by the number of fibrils remaining, but no large change in the details of the particulate fibrillar structures is apparent (Fig. 11). This rules out the possibility that the particulate structure observed at room temperature is due to folded-chain-type crystal overgrowth, since such chain-folded overgrowths are not expected to be stable up to such high temperatures.

Figure 12 shows a film initially stretched 700% at room temperature, conditioned at 75 °C for 10 sec, then cooled to room temperature before OsO_4 staining. Comparison of Fig. 12 with the initial unconditioned texture, Fig. 10, reveals that conditioning leads to improved definition of crystalline nodules and a slight increase in size from about 120 Å for unconditioned samples to 150 Å for conditioned. The short-term application of thermal energy probably allows the system to adjust to nonequilibrium stress distributions imposed by relatively rapid crystallization upon initial stretching. If attempts at conditioning are performed at higher temperatures and for longer periods of time, the structure in general loses contrast and definition, probably due to polymer flow.

Figure 13 shows the effect of gold decoration on a highly stretched film at room temperature. In this case the film has been stretched at room temperature and subsequently conditioned at 75 °C for 10 sec before decorating at room temperature, and stained with OsO_4 after the decoration in order to establish the location of the gold particles with respect to the crystalline-amorphous surface structure. This micrograph shows that atomic gold avoids the crystalline areas of the film resulting in a very selective mapping of surface textural features. A similar decoration pattern is also observed for unconditioned films strained 500 to 700%.

Low temperatures. The effect of holding films strained 500–900% either conditioned or unconditioned, at –28 and +2 °C for various periods of time is shown in Figs. 14 and 15, respectively. At –28 °C distinct changes in the original fibrous structure are apparent after only 1 min, where it is seen that crystalline “growth” perpendicular to the strain axis starts to appear in some areas, resulting in diamond-shaped crystallites. After 3 min at –28 °C, crystalline material with a distinct

lamellar appearance has developed. After 5 min at –28 °C, the emerging lamellar texture is even more pronounced, and after 20 min at –28 °C the transformation to a lamellar texture appears to be essentially complete. In most cases (including those not shown here) the fully developed lamellar texture shows *no evidence* of the original fibrous nodular texture which was originally present over (and filled) large areas of the film. At –28 °C, this lamellar texture exhibits an average periodicity along the strain axis of 140 Å and a crystalline thickness of 55 Å, a value much smaller than the 130-Å crystalline thickness measured at room temperature.

At +2 °C (Fig. 15) a similar transformation to lamellar texture occurs with time, although the rate of this transformation is considerably reduced as compared with holding at –28 °C, taking some 20 h to reach completion. It is of interest to note that the rates of fibrillar-to-lamellar transformation at these two temperatures are surprisingly similar to the rates of stress relaxation for natural rubber at comparable temperatures to be reported in part III. The thickness of the crystalline core at +2 °C is 70–85 Å while the lamellar periodicity is approximately 190 Å, both somewhat larger than at –28 °C. The low temperature fibril-lamellar transformation in films strained 500–900% occurs for both conditioned and unconditioned samples, although conditioned films in general exhibit increased perfection of lamellar development.

In a separate series of experiments, samples were examined in the cold stage of the electron microscope without OsO_4 -staining treatment. Highly strained (700%) samples held 4 h at –28 °C before rapid transferral to the cold stage at –90 °C exhibited an oriented lamellar texture apparently identical to that seen in samples which had been stained. Highly strained samples quenched directly from room temperature into liquid nitrogen before transferral to the cold stage also had an ill-defined lamellar texture (of limited lateral extent) suggesting that the fibrillar-to-lamellar transformation can also occur at very low temperatures.

These results are quite different from those previously reported by Andrews⁴ and later by Andrews and Reeve¹⁷

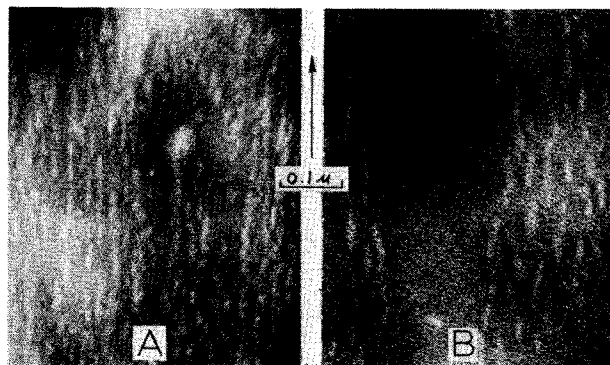


FIG. 11. Natural rubber strained 700%, heated above room temperature and OsO_4 stained at elevated temperature. (a) Heated to 45 °C, 2 min and stained. (b) Heated to 55 °C 2 min and stained.

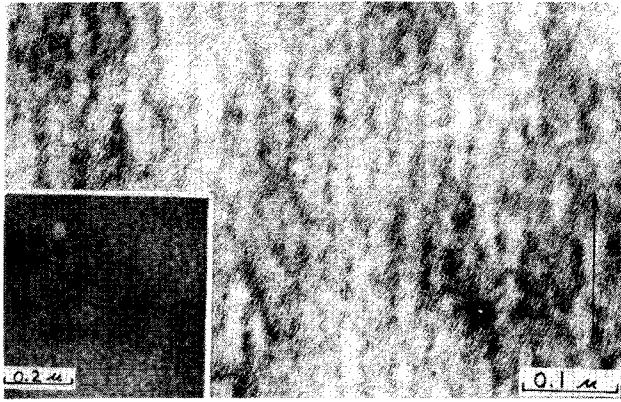


FIG. 12. Natural rubber strained 700% at room temperature, conditioned at 75°C for 10 sec, then cooled to room temperature before OsO_4 staining.

who did not observe any change in the original fibrous morphology when highly strained (700%) films of natural rubber⁴ and polychloroprene¹⁷ were held at low temperatures. Andrews⁴ suggested that the high density of crystallites generated at room temperature at 700% strain prevents further crystalline growth at low temperatures. In the current research, low-temperature lamellae were observed up to the highest elongation of 900%. These observations are supported by small-angle x-ray results which show oriented discrete maxima for samples crystallized under high elongations. However, there is a tendency for lamellar development to become more difficult with increasing elongation, especially above about 700% strain. At 900% strain lamellae generally exhibit poorer contrast and definition and are often intimately mixed with particulate fibrillar structure, apparently unchanged from room temperature.

A number of experiments were performed to further clarify the mechanism of low-temperature fibrillar-lamellar transformation observed in natural rubber films strained 500–900%.

Morphological changes on heating. Natural rubber films strained 700% were held at -28°C to give the lamellar texture and then heated back to room temperature at a rate of $6^\circ\text{C}/\text{h}$. Samples were stained with OsO_4 at temperature intervals of about 7°C in order to preserve the *transient* morphological changes occurring during the heating. Figure 16 presents typical micrographs obtained from such a program. As the temperature reaches -15°C [Fig. 16(b)], the lamellar structures (originally continuous) appear to have broken up into a series of beads aligned perpendicular to the strain axis. As the temperature is further increased, the lamellar structures in general lose definition and contrast. Figure 16(c) shows a typical micrograph obtained from the specimen upon reaching $+2^\circ\text{C}$. Only slight evidence of lamellar texture is found on this sample and the overall texture closely resembles the original room-temperature texture before freezing. The lamellar texture, however, reappears as the sample temperature is further increased. Figure 16(d), the structure at $+8^\circ\text{C}$, exhibits this lamellar reappearance, although this structure is not pronounced. Lamellar texture disappears

rapidly again as the temperature is further increased, and at $+15^\circ\text{C}$ [Fig. 16(e)] only the nodular texture exists and remains visibly unchanged (even with time) as room temperature is reached.

In an experiment related to that described in the preceding paragraph, films strained 700% were crystallized at -28°C to give the lamellar texture and then heated at $6^\circ\text{C}/\text{h}$ to $+2^\circ\text{C}$. This temperature ($+2^\circ\text{C}$) was maintained and the morphology was examined as a function of time. As the temperature reaches $+2^\circ\text{C}$, little evidence of the original lamellar texture which existed at -28°C remains, as expected from the results shown in Fig. 16. However, a lamellar texture reappears with time at $+2^\circ\text{C}$, which is similar to that seen for initial crystallization at $+2^\circ\text{C}$ (Fig. 15). These results also suggest to us that annealing is accompanied by the break up of lamellae into nodules which then recrystallize and rearrange into a lamellar texture with a different crystal thickness. The annealing appears to take longer time for the high-strain than the low-strain samples.

Changes in gold-decoration pattern produced by formation of lamellae at low temperatures. The other experiments concerning lamellar nature and growth involve cooling films strained 700% which had been *previously* gold decorated at room temperature following stretching. After holding at low temperatures for a time sufficient to allow lamellar structure to form, the sample is stained with OsO_4 .

Figure 17 shows a film strained 700%, gold decorated at room temperature following stretching, then held at -28°C . The gold is now aligned perpendicular to the strain axis. Close inspection of such micrographs reveals that the gold particles tend to avoid the lamellar crystalline core and to reside in adjacent amorphous regions as indicated by the osmium staining.

Comparison of Fig. 13 with Fig. 17 showing gold-decoration patterns at room temperature and -28°C , respectively, suggests that the gold originally deposited at room temperature acts as a tracker of material trans-

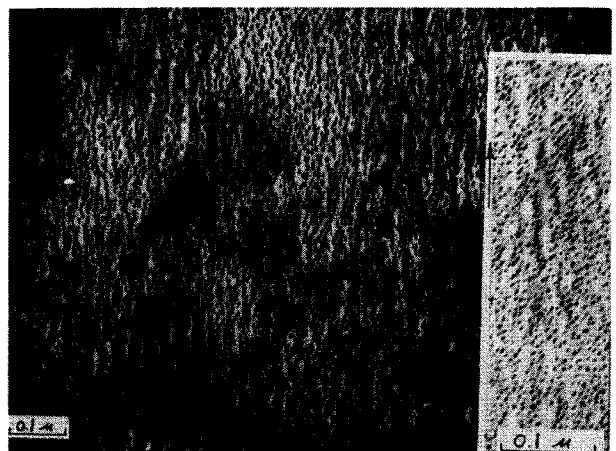


FIG. 13. Natural rubber strained 700% at room temperature, conditioned at 75°C for 10 sec, Au decorated then stained with OsO_4 at room temperature.

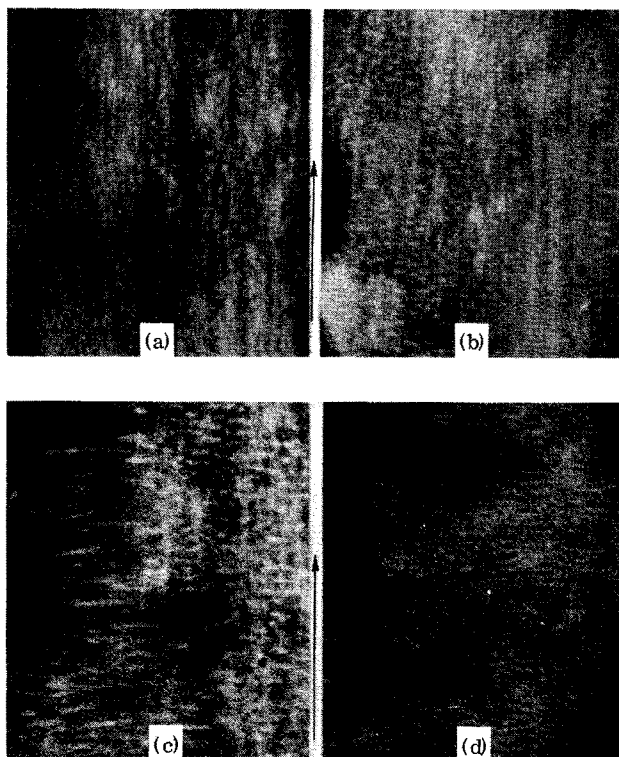


FIG. 14. Natural rubber strained 600% at room temperature, held at -28°C and then OsO_4 stained after various periods of time at -28°C . (a) After 1 min. (b) After 3 min. (c) After 5 min. (d) After 20 min.

port during the low-temperature fibrillar-lamellar transformation.

DISCUSSION

Several important findings have resulted from this series of detailed electron microscope studies of natural rubber thin films prepared under a variety of experimental conditions. These include (a) observation of nearly aligned crystalline nodules some 100 to 150 Å in size parallel to the stretch direction when films are strained more than about 250% at room temperature, thus giving rise to the appearance of *discontinuous* fibrils about 100 Å in diameter; (b) formation of crystalline lamellae for all elongations up to 900% when films are held at low temperatures for sufficient time, the number of lamellae per unit area being larger at lower temperatures; (c) a thermally reversible fibrillar-to-lamellar transformation in films strained greater than 250%, the transformation being faster at lower temperatures and more difficult at higher extensions; (d) the observation that subsequent cooling of either strained or unstrained specimens, but which have been previously gold decorated at room temperature, results in a tendency for the gold particles to reside along the edges of crystalline lamellae suggesting that the formation of lamellae involves the same Au-voided regions seen at room temperature (containing crystallized or uncrystallized nodules); (e) evidence for nodular structure within crystalline lamellae; and (f) evidence for an elementary nodular structure in unstretched amorphous molten natural rubber having a characteristic size of approximately 100 to 150 Å.

Formation of crystalline nodules at room temperature in films strained greater than 250%—strain-induced crystallization

Regardless of the degree of elongation (250–900%) the strain-induced crystallites developed at room temperature all have growth restricted to less than 150 Å in size, although their population density clearly increases with increased elongation. There are a number of possibilities for the origin of the texture.

(i) The crystallites might consist of micellar-type extended-chain crystals but are restricted in growth due to the rapidity of crystallization, a postulate appearing to be consistent with the extremely rapid rates of strain-induced crystallization of rubber at room temperature.²⁷ One would then expect subsequent crystal growth to occur more readily along the *c* axis, resulting in an increase in crystallite size in the stretch direction. Experimentally this is not observed. Instead lamellar-type crystals of *thinner* crystalline core are observed in all extensions up to 900% when further crystal growth is allowed to occur at low temperatures.

(ii) The nodular texture results from folded-chain crystalline growth onto a central hidden extended-chain backbone. A number of observations contradict this postulate. First, the nodular crystallites usually appear isolated, including evidence from dark-field electron microscopy, with no evidence of an extended-chain backbone of any reasonable diameter that can still be considered a crystal. (Discontinuous-type fibrils have also been established by dark-field electron microscopy previously by Yeh and Geil in polyethylene terephthalate,² Yeh and Lambert in isotactic polystyrene,¹⁶ and Klement and Geil in several other polymers crystallized under orientation.²⁸) Second, heating above room temperature does not affect the lateral dimension of the nodules. Third, although the crystalline nodules appear to align along lines parallel to the stretch direction, at high magnifications they often exhibit a random spatial distribution, again questioning the postulation of any extended-chain nuclei of reasonable extended lengths along the *c*

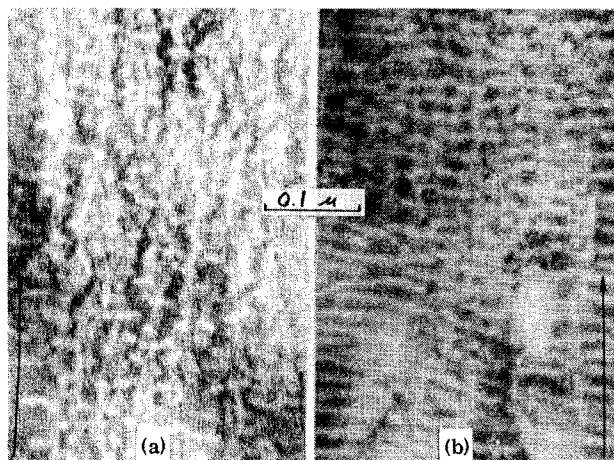


FIG. 15. Natural rubber strained 600% at room temperature, held at $+2^{\circ}\text{C}$ and then OsO_4 stained after various periods of time at $+2^{\circ}\text{C}$. (a) After 4 h. (b) After 20 h.

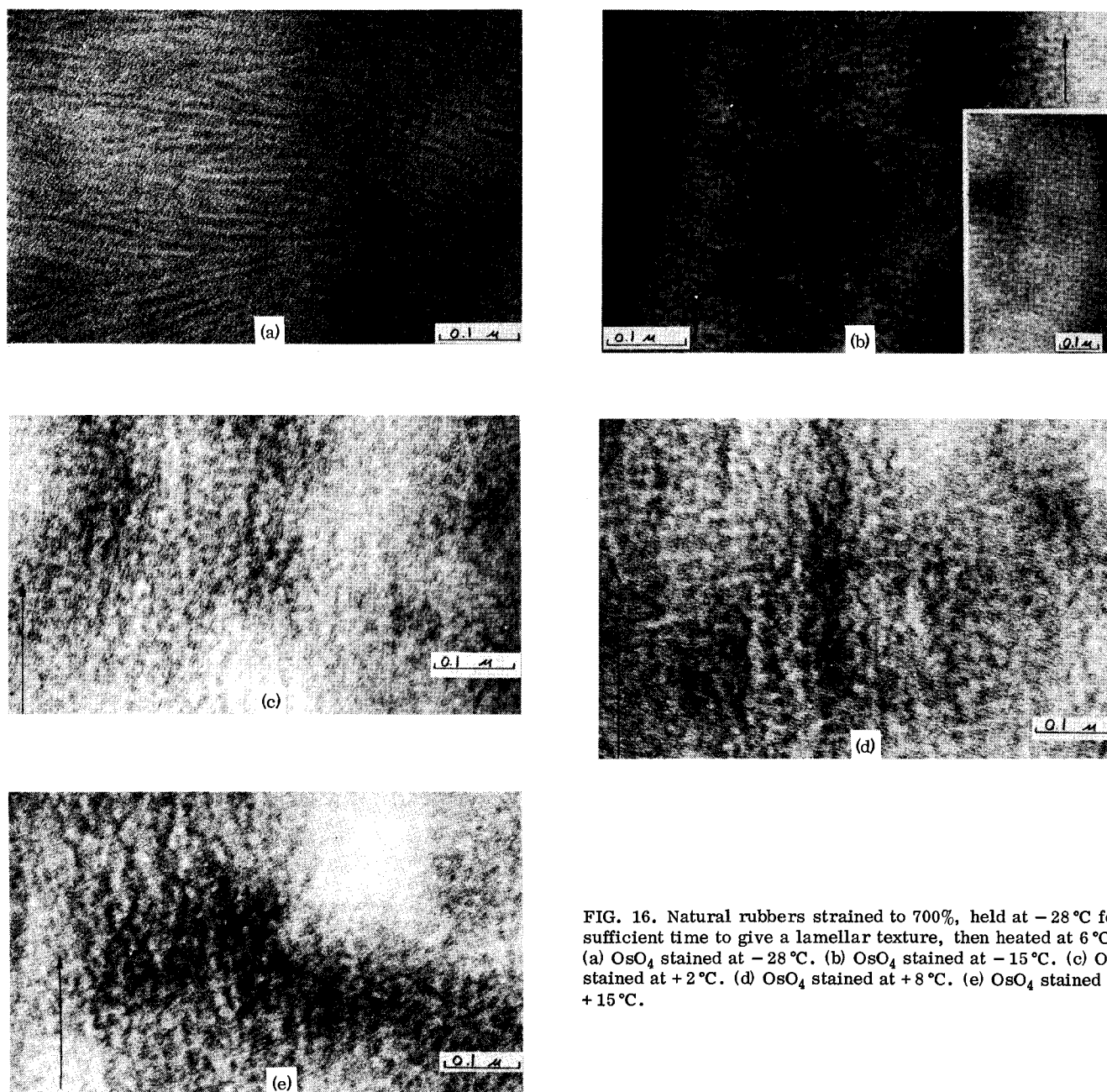


FIG. 16. Natural rubbers strained to 700%, held at -28°C for sufficient time to give a lamellar texture, then heated at $6^{\circ}\text{C}/\text{h}$. (a) OsO_4 stained at -28°C . (b) OsO_4 stained at -15°C . (c) OsO_4 stained at $+2^{\circ}\text{C}$. (d) OsO_4 stained at $+8^{\circ}\text{C}$. (e) OsO_4 stained at $+15^{\circ}\text{C}$.

axis. Finally, crystalline growth by chain folding would result in an increase in axial stress. This is in fact never observed during oriented crystallization of natural rubber at room temperature.

(iii) The only other apparent possibility is that the crystallites arise by alignment and crystallization of partially chain-folded nodules preexisting in the unstrained melt, similar to the mechanism previously deduced from detailed morphological studies of strain-induced crystallization of polyethylene terephthalate from the glassy state.² This conclusion is further substantiated by the results obtained in this study of platinum shadowing, gold decoration, and OsO_4 staining of unstretched films at room temperature, indicating structure with size similar to the rapid strain-induced room-temperature crystallites.

Development of lamellae at low temperatures—fibrillar-to-lamellar transformation

The present electron microscopy investigation has also shed considerable light on the formation of lamellae observed at low temperatures for all elongations studied.

Characteristics of lamellae

Table I summarizes the characteristic dimensions of crystalline textures seen in this work. The first column gives the strain and the holding temperature at which the film is stained, while column 2 gives the observed crystalline texture. The crystal thickness, column 3, reports the lamellar, or (in the case of high strain, room-temperature nodular crystallites) the unstained nodular diameter. The amorphous thickness, column 4, is the thickness of the stained region between crystalline la-

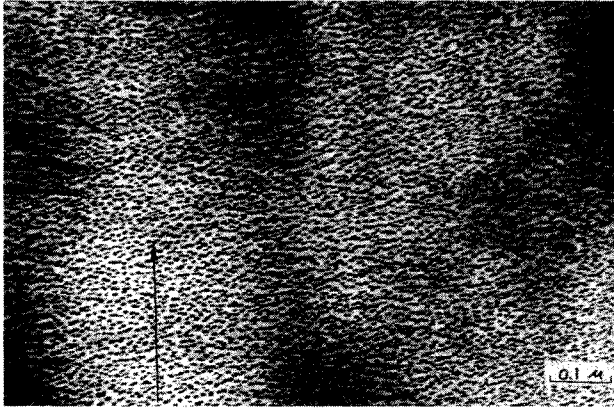


FIG. 17. Natural rubber strained 700% at room temperature. The film was Au decorated at room temperature, held at -28°C to develop lamellar texture and then OsO_4 stained at -28°C .

mellae. This amorphous thickness generally shows large variation on any particular sample, but is presented to indicate general trends, and in general its value is *larger* than its corresponding crystalline thickness. The axial periodicity of column 5 is the average sum of amorphous and crystalline thickness, determined by randomly drawing lines coincident with the strain axis and dividing a given linear distance by the number of repeats contained in this distance.

The measurements indicate that both the crystal thickness and periodicity appear to be rather insensitive to elongation at a particular temperature. However, the lamellar periodicity increases noticeably with increasing temperature, reflecting the sum of increases in both crystalline thickness and amorphous thickness. Within experimental error, there appears to be a *proportional* increase in crystalline thickness, amorphous thickness, and periodicity with increasing temperature. This indicates that the *difference* between the crystalline and the amorphous regions will be *proportionally greater* at higher and higher temperatures (since the thicknesses of the crystalline regions are smaller and amorphous regions are larger to begin with). This is an important observation which will be discussed further in part II. The crystalline thicknesses reported here are in general agreement, although somewhat smaller, with similar measurements of lamellar crystalline thickness in unstretched natural rubber films recently reported by Andrews, Owen, and Singh.²⁹ They did not report any measurements for either the amorphous thickness or the periodicity between lamellae.

Mechanism of lamellar formation

In considering the possible mechanisms for low-temperature lamella formation, it is convenient to consider first strains of greater than about 250%, for which crystalline nodules appear at room temperature. The conclusions reached for the high-strain material will then be related to lower elongations.

Possibility of a nucleating thread. Keller and Machin suggest that the oriented lamellar texture in strain-crystallized polymers is a direct result of epitaxial folded-chain crystallization onto a line nucleus coinci-

dent with strain. It might be suggested that room-temperature strain-induced crystalline nodules serve as such line nuclei. Indeed, nodular crystals generated by stretching at room temperature often appear to show some alignment in strings of nodules, and at low temperatures lamellar growth often appears to emanate from such strings of nodules. However, as noted earlier, very often the strain-induced crystalline nodules and lamellar growth sites exhibit locational randomness. Furthermore, the fully developed lamellar texture shows no evidence of the original room-temperature nodular texture which covers nearly 50% of the total area in highly stretched samples. These observations clearly question the necessity of a line nucleus to explain the observation of a stack of oriented lamellae; a common orientation of the nodules brought about by the stretching process in the rubbery state is all that is needed for subsequent development of oriented lamellae.

Role of the room-temperature nodular crystallites in lamellar formation. An important question remains concerning the relationship of the strain-induced crystalline nodules seen at room temperature and the lamellar structures which develop at lower temperatures. Two possible roles can be visualized for the nodules in the transformation to lamellar texture.

(i) A complete recrystallization may occur in which all memory of the original nodules is lost in the transformation to lamellar texture. Although in most cases the lamellar structure exhibited little evidence of the original crystalline nodules, a complete recrystallization appears unlikely based on two observations. First, lamellar development in samples strained 700% produces a very characteristic pattern of gold decoration, even though the original decoration was performed at room temperature where only nodules were present (compare Figs. 13 and 17). This indicates that the nodular structures, originally voided of gold, become somehow incorporated into the crystalline lamella, also voided of gold, and in so doing maintain some semblance of their original identity. Second, the fact that the nodular-lamellar transformation is thermally reversible, in that the lamellar structure will transform back to a nodular texture upon reheating to room temperature (Figs. 9 and 16), suggests that the lamellae retain some memory of the original nodular texture.

(ii) The other possibility for the role of the nodular structure in the formation of lamellae, which is supported by gold decoration and reversibility observations discussed in the preceding paragraph, is that the original room-temperature crystallites become intimately incorporated into the lamellae, maintaining a semblance of their identity. The possible mechanisms by which this might occur will be discussed next.

Possible mechanisms of low-temperature fibrillar-to-lamellar transformation: 500-900% strain

Several possibilities may exist for the transformation from nodular to lamellar texture.

The simplest case would be a mere translation and coalescence of crystalline nodules into a lateral array. However, this must be an oversimplification for two reasons. First, both wide-angle electron and x-ray (part II)

TABLE I. Characteristic dimensions of crystalline textures.

Strain (%) / crystallization temperature, time	Crystal texture	Thickness (Å)		Lamellar periodicity (Å)
		Crystal	Amorphous	
0% / +5 °C, 15 days	Lamellar	60–85 (75) ^a
	Noncrystal- line nodular	70–150 ^b (110)		
0% / -28 °C, 13 h	Lamellar	45–75 (60)
100% / +5 °C, 15 days	Lamellar	65–80 (75)	120–165 (125)	200–230 (200)
100% / -28 °C, 1 day	Lamellar	45–60 (55)	70–115 (80)	130–160 (140)
300% / -28 °C, 1 h	Lamellar	45–65 (55)	50–105 (80)	120–150 (135)
700% / +2 °C, 20 h	Lamellar	70–85 (80)	80–110 (100)	180–210 (190)
700% / -28 °C, 20 min	Lamellar	45–65 (55)	55–95 (75)	120–150 (140)
700% / +28 °C: Uncondi- tioned	Nodular	100–130 ^b (120)
Conditioned	Nodular	120–160 ^b (150)

^a Most probable size in brackets.

^b Measurement made of unstained nodular diameter.

diffraction patterns as well as electron micrographs indicate some increase in crystallinity (or crystalline regions) for the low-temperature lamellar texture as compared with the room-temperature fibrillar texture, even at the highest strains of 700% for x-ray samples (part II) and 800–900% for electron microscopy thin-film samples. This extra crystallinity probably results from additional crystallization of nodules which have not crystallized at room temperature together with crystallization of material between the nodules. The second reason is that the room-temperature nodules have an approximate diameter of 120 Å for unconditioned and 150 Å for conditioned samples, while the thickness of the crystalline lamellar core is less than 80 Å at +2 °C and at -28 °C is about 55 Å (Table I). Osmium staining and gold decoration both give independent verification of these measurements. This means that if the nodular crystals are to be incorporated into the lamellar crystal, either they must melt back parallel with the strain axis or they must re-fold to shorter fold lengths.

The postulate that nodular fold-chain crystallites melt back upon cooling and simultaneously laterally align is not only thermodynamically unreasonable but is also accompanied by the same difficulties advanced for the original fringed micelle model, notably the steric hindrance associated with traversing a planar boundary from a highly ordered crystalline region to a disordered lower-density amorphous region. Although the chains

would still be folded back into the crystal, they would be long loops and the situation would approach the bundle-type fringed-micelle model. It might be argued that such steric problems would exist only over a relatively small planar area of approximately $100 \times 100 \text{ \AA}^2$ based on the initial nodular dimensions, and that planar continuity could be achieved by a folded-chain-type crystallization in the internodular regions thus alleviating the steric problems somewhat. However, in order for this to occur the internodular material would also have to be prefolded because the results of stress relaxation (part III) show that the axial stress decays to zero during the fibrillar-to-lamellar transformation, a result inconsistent with epitaxial chain-folded crystallization in the normal sense of reeling in of randomly coiled chains, which will result in a stress rise.

The second possibility for decrease in axial crystalline thickness during incorporation of nodules into lamellae is for the nodular crystal to *refold* to a lower fold length, and in so doing transform dimensionally to anisotropic platelets whose thickness is characteristic of the holding or subsequent crystallization temperature. Minor translations of these platelets, combined with some additional crystallization of previously uncrystallized nodular and/or internodular material would result in the observed coherent lamellar texture with a much reduced total crystalline surface area, resulting in a thermodynamically more favorable state. Possible refolding of chains within the crystalline nodules is supported somewhat by the fact that short-term (30-sec) exposure of films strained 700% at -28 °C results in almost complete loss of crystalline-amorphous contrast (as revealed by OsO₄ staining), an observation that seems difficult to explain in any other way.

At strains less than about 200%, no crystalline structure is detected at room temperature, in accord with previous studies.^{4,14} The low-temperature lamellae for 0–200% strain are similar to those observed at higher elongations. This suggests that the crystalline lamellae in films strained less than 200% may also be composed of partially folded nodules, not crystalline at room temperature, but which crystallize and align during lamellar development at low temperature.

Evidence for elementary nodular structure in natural rubber melts

As pointed out earlier, a convincing piece of evidence pointing to the existence of a melt structure is the appearance of strain-induced crystallites after rapid stretching at room temperature which have a size similar to that of structures seen in unstretched films. The similarity of the low-temperature lamellar structures for high and low strain is further evidence connecting the high-strain room-temperature crystalline nodules with the postulated melt structure. Further evidence, in addition to that from dark-field studies,²² supporting melt structurization is the result of crystallization of unstretched natural rubber films which have been previously gold decorated at room temperature. In selected areas where the lamellae have formed having edgewise orientation with the film plane, the gold shows a definite tendency to outline the edges of the lamellar crystals (Fig. 6). This observation cannot be taken as positive

proof of a relationship between lamellar structure and the voided regions seen at room temperature because of the unsolved nature of gold decoration and possibility that the gold particles could be excluded from the surface of the crystalline lamellar core due to some undefined mechanism. However, the observation is certainly consistent with the postulated melt structure and its relationship with the lamellar crystals.

CONCLUSIONS

(i) A number of independent techniques suggest the presence of elementary partially folded noncrystalline nodules (~ 100 – 150 Å) in natural rubber melts.

(ii) Stretching natural rubber thin films greater than about 250% at room temperature results in the orientation and crystallization of nodules, about 120 Å in size. Although the population density of these crystallites increases with increased elongation, their size remains unaltered within the error of measurement. Short-term application of thermal energy by conditioning results in increased perfection and size (150 Å) of these room-temperature nodules.

(iii) Holding natural rubber films at low temperatures (-28 to about $+15$ °C in this research) results in formation of lamellae for strains of 0–900%. In samples strained 100% or more, the lamellae are highly oriented perpendicular to the stretch direction and are normally seen edgewise to the film plane. No central nucleating threads appear necessary for the development of this oriented lamellar texture. In unstretched films lamellae can have both perpendicular and planar orientation with the film. The crystalline lamellae are characterized by significant chain folding.

(iv) At elongations of greater than 250%, the low-temperature transformation to a lamellar texture involves intimate incorporation of room-temperature crystalline nodules into the lamellar crystals, resulting from small translations of the nodular units and lateral alignment. Judging from electron diffraction spot intensities, the transformation is always accompanied by an increase in degree of crystallinity even at the highest strains of 800–900%. This is probably due in part to crystallization of internodular matrix material to supply crystallographic coherency between neighboring nodules and in part to crystallization of those nodules which had not

crystallized at room temperature. Incorporation of the room-temperature nodular crystallites into lamellae is accompanied by a decrease in the axial crystallite dimension, probably by means of a refolding mechanism.

(v) At all elongations, lamellae formed at increasing temperature are characterized by slightly increased crystal thickness (55 Å at -28 °C to 75 Å at $+5$ °C), increased lamellar periodicity (140 Å at -28 °C to 200 Å at $+5$ °C), increased contrast (as determined by OsO₄ staining), and a decrease in number of lamellae per unit area.

(vi) The fibrillar-to-lamellar transformation is reversible with temperature at all elongations.

ACKNOWLEDGMENT

Acknowledgment is made to the donors of the Petroleum Research Fund, administered by the American Chemical Society, for support of this research.

*Present address: Research Center, International Nickel Company, Sterling Forest, Suffern, N. Y. 10901.

¹A. Keller and M. J. Machin, *J. Macromol. Sci. Phys.* **1**, 41 (1967).

²G. S. Y. Yeh and P. H. Geil, *J. Macromol. Sci. Phys.* **2**, 251 (1967).

³K. Kobayashi, reported by P. H. Geil in *Polymer Single Crystals* (Interscience, New York, 1963).

⁴E. H. Andrews, *Proc. R. Soc. A* **277**, 562 (1964).

⁵A. J. Pennings and A. M. Kiel, *Kolloid-Z.* **205**, 160 (1965).

⁶T. Kawai, K. Ebara, and H. Maeda, *Kolloid-Z.* **229**, 168 (1969).

⁷F. M. Willmouth, A. Keller, I. M. Ward, and T. Williams, *J. Polym. Sci. A* **6**, 1627 (1968).

⁸D. Krueger and G. S. Y. Yeh, *J. Macromol. Sci. Phys.* **6**, 431 (1972).

⁹G. S. Y. Yeh (unpublished).

¹⁰A. N. Gent, *Trans. Faraday Soc.* **50**, 521 (1954).

¹¹A. N. Gent, *J. Polym. Sci. A* **4**, 447 (1966).

¹²G. Grespi, U. Flisi, and U. Arcozzi, *Chim. Ind. (Milan)* **44**, 627 (1962).

¹³A. N. Gent, *J. Polym. Sci. A* **3**, 3787 (1963).

¹⁴G. S. Y. Yeh, General Tire and Rubber Co. Research Report, 1963 (unpublished).

¹⁵G. S. Y. Yeh and P. H. Geil, *J. Macromol. Sci. Phys.* **1**, 235 (1967).

¹⁶G. S. Y. Yeh and S. L. Lambert, *J. Appl. Phys.* **42**, 4614 (1971).

¹⁷E. H. Andrews and B. Reeve, *J. Mater. Sci.* **6**, 547 (1971).

¹⁸D. Luch, Ph.D. thesis (University of Michigan, 1971) (unpublished).

¹⁹G. A. Bassett, D. J. Blundell, and A. Keller, *J. Macromol. Sci. Phys.* **1**, 161 (1967).

²⁰B. J. Spit, *J. Macromol. Sci. Phys.* **2**, 45 (1968).

²¹S. Lambert, Ph. D. thesis (University of Michigan, 1970) (unpublished).

²²G. S. Y. Yeh, *J. Macromol. Sci. Phys.* **6**, 451 (1972).

²³K. H. Storcks, *J. Am. Chem. Soc.* **60**, 1753 (1938).

²⁴L. A. Wood and N. Bekkedahl, *J. Appl. Phys.* **17**, 362 (1946).

²⁵E. H. Andrews, *J. Polym. Sci. A* **4**, 66 (1966).

²⁶S. D. Gehman and J. E. Field, *J. Appl. Phys.* **10**, 564 (1939).

²⁷J. C. Mitchell and D. J. Meier, *J. Polym. Sci. A* **6**, 1689 (1968).

²⁸J. J. Klement and P. H. Geil, *J. Macromol. Sci. Phys.* (to be published).

²⁹E. H. Andrews, P. J. Owen, and A. Singh, *Proc. R. Soc. (Lond.) A* **324**, 79 (1971).